

RSC Pharmaceutics

Accepted Manuscript

This article can be cited before page numbers have been issued, to do this please use: M. Sharma and N. Gupta, *RSC Pharm.*, 2025, DOI: 10.1039/D4PM00327F.



This is an Accepted Manuscript, which has been through the Royal Society of Chemistry peer review process and has been accepted for publication.

Accepted Manuscripts are published online shortly after acceptance, before technical editing, formatting and proof reading. Using this free service, authors can make their results available to the community, in citable form, before we publish the edited article. We will replace this Accepted Manuscript with the edited and formatted Advance Article as soon as it is available.

You can find more information about Accepted Manuscripts in the [Information for Authors](#).

Please note that technical editing may introduce minor changes to the text and/or graphics, which may alter content. The journal's standard [Terms & Conditions](#) and the [Ethical guidelines](#) still apply. In no event shall the Royal Society of Chemistry be held responsible for any errors or omissions in this Accepted Manuscript or any consequences arising from the use of any information it contains.

Tailoring of bromelain loaded lipid polymer hybrid nanoparticles for asthma management: Fabrication and preclinical evaluation

View Article Online
DOI: 10.1039/D4PM00327F

Manu Sharma,* Namita Gupta

Department of Pharmacy, Banasthali Vidyapith, Rajasthan, India-304022



Corresponding Author

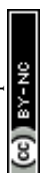
Dr. Manu Sharma
Associate Professor
Department of Pharmacy
Banasthali Vidyapith,
Banasthali Rajasthan, India-304022
Mobile no. +91-9001701324
Email: aasmanu2018@gmail.com; sharmamanu10@gmail.com

Abstract

View Article Online
DOI: 10.1039/D4PM00327F

Poor response along with associated side effects of available drugs in clinics has limited the successful asthma management. Traditionally, bromelain has been found effective in asthma management. However, high oral dose and poor bioavailability limits its use. Therefore, present investigation was tailored to prepare bromelain loaded lipid polymer hybrid nanoparticles (Br-LPHNs) to enhance oral bioavailability and therapeutic efficacy of bromelain in allergic asthma management. Br-LPHNs having a lipid core encapsulated in biomimetic polymethylmethacrylate coat were prepared utilizing double emulsion solvent evaporation method. Drug release behavior, mucolytic potential and stability of optimized formulation were evaluated. Pharmacokinetic and pharmacodynamic studies were executed in allergen-induced asthma model. Optimized Br-LPHNs manifested nanosize (190.91 ± 29.48 nm) and high entrapment efficiency ($89.94 \pm 3.98\%$) with gastro-resistant and sustained drug release behavior upto 24h. LPHNs as carrier improved shelf life (~ 6.99 -fold) and bioavailability (6.89 -fold) relative to neat bromelain. Optimized formulation significantly suppressed bronchial hyperresponsiveness, delayed bronchospasm induction and reduced spasm severity. Moreover, oxidative and immunological markers were significantly ($p < 0.05$) diminished along with restoration of antioxidant enzyme to normal level. Histopathological investigations also assured reduced tissue injury. Thus, Br-LPHNs development not only ensured in-vitro and in-vivo bromelain stability but also offered a promising option for managing asthma.

Keywords: Airway hyper-responsiveness; Bromelain; Hybrid nanoparticles; Inflammation; Asthma.



Introduction

View Article Online
DOI: 10.1039/D4PM00327F

Asthma is a complicated and multifactorial chronic inflammatory respiratory illness with complex pattern of inheritance.^{1,2} It is characterized by multicellular inflammation, bronchospasm, airway obstruction and hyper-responsiveness of airways associated with episodes of wheezing and spasmodic coughing often worsening at night. Asthma is customarily immortalized in response to peculiar as well as panoramic triggers.³ The majority of the reversible or permanent pathophysiological alterations in the airway wall occurring during asthma are caused by the acute activation and accumulation of inflammatory cells, increased helper T cell expression, dysplasia of the goblet cells and airway muscles, and changes in the quantity and quality of mucus production.⁴ Thus, a cascade of events occurring at molecular level generates oxidative environment which impairs antioxidant defense of lungs and facilitates destruction of macromolecules.⁵

Current medications like inhaled β -agonists and glucocorticoids are among best therapies for asthma management. These treatments can reduce airway inflammation, ease bronchoconstriction, and improve quality of life for many patients but fail to address the structural abnormalities provoked by the disease. In addition, long-term use can lead to serious side effects, such as high blood pressure, cataracts, osteoporosis in older adults, and slowed growth in children.^{6,7} Furthermore, a sizable portion of people continue to not respond well to these medications, resulting in inadequate asthma management.⁸ Therefore, a crucial need exist to explore new novel alternative therapies for asthma in the clinic. Scientists and pharmaceutical researchers are paying particular attention to the growing interest in herbal therapies for managing asthma because of the encouraging results of clinical and experimental trials.^{9,10}

In traditional system of medicine, bromelain has potential pleiotropic therapeutic benefits as mucolytic,¹¹ wound healing,¹² fibrinolytic,¹³ antithrombotic,¹⁴ anti-inflammatory,¹⁵



antioxidant,¹⁶ anticancer¹⁷ as well as immunomodulatory agent.¹⁸ According to earlier studies, bromelain effectively lowers airway reactivity and irritant susceptibility in ovalbumin-induced allergic airway illness by lowering the levels of lung inflammation markers.^{19,20} Bromelain also impairs cyclooxygenase-2 and prostaglandin E2 expression and diminishes cytokines production activated during inflammatory conditions.^{21,22} Downregulation of inflammation is further aided by bromelain's proteolytic breakdown of cell surface signals, which synchronizes lymphocyte homing and movement to the inflammatory location.²³ Furthermore, bromelain synchronizes expression of transforming growth factor (TGF)- β , a paramount regulator of inflammation.²⁴ However, high dose, poor shelf-life, mechanical and gastric instability restricts its therapeutic prospective. The vulnerability of bromelain to degrade, denature or agglomerate in gastric environment may correspond to uncertain prophylactic hypersensitivity or toxic reactions along with loss of therapeutic effect.^{15,25} This warrants the exploration of novel formulation approaches to foster the development of sturdy and patient compliant oral bromelain therapy for asthma management.

Nano-scale carriers in the field of nanomedicines have gained wider attention in evolution of novel formulations of protein and peptides. Polymeric nanoparticles, solid lipid nanoparticles and liposomes have received attention to great extent among nanocarriers to amplify the absorption over the GIT via distinct absorption mechanisms.²⁶⁻²⁸ It is notably challenging to encapsulate bromelain, a hydrophilic molecule in polymer or lipid based nanocarriers due to its quick partitioning to aqueous phase at the time of development. Instead, liposomes have enormous prospective of encapsulating hydrophilic drugs. However, inconsistent and uncertain absorption of liposomes along with their insufficiency to maintain structural integrity at absorption site limits their oral delivery.²⁸ Therefore, to overcome the restrictions of prevailing systems, lipid polymer hybrid nanoparticles (LPHNs) based robust design has been endorsed having a lipid core enveloped in polymeric layer. The lipid core hinders



partitioning of hydrophilic drug by forming molecular barrier to aqueous system while polymeric layer confirms the structural integrity and biomimetic shield. Numerous reports are available in literature confirming fabrication of LPHNs for hydrophilic drugs inspite of polymeric nanocarriers.^{29,30} The use of polymethylmethacrylate (PMMA), a pH sensitive polymer also has an add on effect of protecting proteins / enzymes from acidic milieu of stomach and mimicking drug release in intestine.³¹ Moreover, core-shell architecture of LPHNs hampers inward permeation of gastro-intestinal fluid facilitating prolonged drug release. The distinctive characteristics of LPHNs like nanosize facilitating quick stomach emptying, increased surface area, site-specific controlled delivery, enhanced cellular absorption, reduced first pass metabolism and adverse or toxic effects, enhanced bioavailability and improved patient compliance has increased their acceptance in delivering the challenging molecules like proteins.^{29,30} To best of our comprehension, no reports are available in literature regarding the formulation of bromelain loaded LPHNs (Br-LPHNs).

Henceforth, present study was undertaken to develop and optimize Br-LPHNs using lecithin as lipid and PMMA as a polymer. Furthermore, optimized nanoparticulate formulation was analyzed for its release behavior, stability, pharmacokinetics and anti-asthmatic activity in guinea pigs as animal model.

Experimental

Materials

Poly methyl (methacrylate) (100.12 g/mol), bromelain, casein, tyrosine and trichloro acetate (98.0%) were procured from Himedia laboratory Pvt. Ltd, Mumbai, India. Polyvinyl alcohol (PVA) and mannitol were purchased from S.D fine Chemicals Ltd, Mumbai. Dichloromethane (DCM) was received from Merck, Germany. All other chemicals and solvents were of analytical grade and were used without further purification. Double distilled water was used throughout the study.



Fabrication of Br-LPHNs

View Article Online
DOI: 10.1039/D4PM00327F

Br-LPHNs were prepared utilizing double emulsion solvent evaporation technique with slight modification.¹⁴ Bromelain and soya lecithin co-dissolved in tris HCl buffer (pH 5.0) constituted aqueous phase. Primary emulsion (w/o) was formed by the dropwise addition of aqueous phase to the organic phase while being sonicated (20 W power, 20% amplitude) for 7 minutes at 4 °C. The organic phase was made up of PMMA dissolved in dichloromethane with a surfactant (0.5 % w/w, Span 80). The primary colloidal dispersion was further emulsified by adding dropwise in aqueous PVA (1 % w/v) under probe sonication at 4 °C. The resulting double emulsion was then agitated at room temperature (100 rpm, 12 h) to enable complete removal of organic solvent. To get rid of free bromelain and unused surface-active agent, nanoparticulate dispersion was centrifuged at 22,000 rpm for 15 minutes at 4 °C followed by washing twice with distilled water. Finally, recovered nanoparticles pellet was dispersed in mannitol solution (10 % w/v) and lyophilized. Ultimately, the pellet of recovered nanoparticles was distributed in a cryoprotectant solution containing 10% w/v mannitol. Lyophilized formulations were stored in air tight container at 4 °C to execute further examinations. Various process variables like lipid and polymer concentration, drug loading, volume of continuous phase along with sonication time were optimized to achieve formulation of nano size range, high entrapment efficiency and good colloidal properties (Table 1).

Characterization of Br-LPHNs

Particle size, polydispersity index (PDI) and zeta potential

The average particle size, PDI and zeta potential of prepared Br-LPHNs was estimated utilizing Nano ZS (Malvern, Germany). Samples were dispersed in double distilled water and suitably diluted prior to estimation.



Entrapment efficiency

View Article Online
DOI: 10.1039/D4PM00327F

Briefly, clear supernatant collected after centrifugation at 22,000 rpm for 15 minutes at 4 °C of nanoparticulate formulations before lyophilization was suitably diluted prior to analysis for free bromelain content by Lowry method using U.V. /Vis spectrophotometer (LabIndia® UV 3000+, Mumbai, India) at 750 nm.³² Entrapment efficiency (EE) was determined by formula:

$$EE (\%) = \frac{\text{Amount of bromelain added} - \text{amount of bromelain in supernatant}}{\text{Amount of bromelain added}} \times 100 \quad (i)$$

Morphology

Field emission scanning electron microscopy was utilized to analyze the morphology of lyophilized materials. Lyophilized samples were mounted on aluminum stubs using carbon adhesive tape and observed at a working distance of 30 mm and an acceleration voltage of 5 KV with subsequent capturing of images.

Structural integrity

The conformational integrity of bromelain in freeze dried nanoparticles was analyzed qualitatively using fluorescence spectrometer (Perkin Elmar LS-45). Freeze dried formulation equivalent to 1 mg bromelain was dispersed in dichloromethane to lyse the vesicles and centrifuged at 22,000 rpm at 4 °C. Pellet collected was dissolved in distilled water and analyzed by fluorescence spectrometer to acquire the emission spectrum (250-500 nm) of samples at an excitation wavelength of 280 nm and a scan rate of 100 nm min⁻¹. The correction in each protein spectrum was done by subtracting the spectrum of blank solution.³³

Consecutively, pure drug and lyophilized optimized formulation was subjected to different pH ambience i.e., pH 1.2 and 6.8 equivalent to stomach and small intestine respectively to envisage their firmness in gastro-intestinal tract. In detail, precisely weighed pure drug and



Br-LPHNs nanoparticles equivalent to 2 mg bromelain were dispersed in HCl buffer pH 1.2 and phosphate buffer pH 6.8 respectively followed by incubation at 37 ± 0.5 °C and 100 shakes per minute for 2 h. The substantial effect of respective condition after incubation on conformational integrity of bromelain was determined qualitatively using fluorescence spectrometer.

Dissolution profile

In vitro bromelain release from Br-LPHNs was evaluated utilizing dialysis membrane method.¹⁶ Dialysis sac containing Br-LPHNs (equivalent to 50 mg bromelain) was dipped in pH progressive dissolution media (100 ml, HCl buffer pH 1.2 for 2 h followed by phosphate buffer pH 6.8) kept at 37 ± 2 °C under 100 rpm. Aliquots (2.5 ml) withdrawn at regular time intervals up to 24 h were restored with same volume of respective buffer after each withdrawal and analyzed at 750 nm for protein content spectrophotometrically.

Mucolytic activity

The artificial mucous having viscoelastic behavior similar to human airway mucus was prepared by mixing locust bean gum (1% w/v) slowly in preheated sodium nitrite solution (1% w/v) at 80 °C followed by continuous stirring at magnetic stirrer for 24 h. Losses in volume occurring due to evaporation were adjusted by adding sufficient amount of sodium nitrite solution whenever required. The galactomannan chains in locust gum bean solution were cross linked by addition of 0.1 M sodium tetraborate.³⁴ The resultant mucous (2 gm) was incubated at 37 °C in an orbital shaker at 100 rpm with drug (0.2 % w/w) and Br-LPHNs dispersion (equivalent to 0.2 % w/w bromelain) respectively. The comparative evaluation of effect of drug and Br-LPHNs dispersion on viscoelastic properties of artificial mucous was determined at predetermined time interval of 2, 4, 6, 8 and 24 h using Rheometer (Brookfield D 220, USA) at 25 °C.



Stability studies

View Article Online
DOI: 10.1039/D4PM00327F

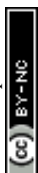
Pure drug and lyophilized formulation were assessed for their stability as per ICH guidelines to determine their suitable storage condition and shelf-life. Samples sealed in airtight amber colored glass vials were stored at accelerated temperature ($40 \pm 2^\circ\text{C}$ / $75 \pm 5\%$ RH) and room temperature ($25 \pm 2^\circ\text{C}$ / $60 \pm 5\%$ RH) storage conditions for 6 and 12 months respectively. At definite time gaps (0, 1.5, 3, 6, 9 and 12 month), samples were withdrawn and evaluated for percentage proteolytic activity of bromelain remaining respectively.¹⁵

In vivo studies

Current animal study performed was duly approved by Banasthali Vidyapith IAEC (574/GO/ReBi/S/02/CPCSEA), in obedience with the guidelines of CPCSEA, Ministry of Social Justice and Empowerment, Government of India. Adult guinea pigs (300–450 g) and wistar rats (220 ± 20 g) of either sex were used for animal studies. Animals were housed with free access to pelleted food and water *ad libitum* under light-dark cycle of 12 h each at $22 \pm 1^\circ\text{C}$ and $55 \pm 5\%$ RH throughout the study.

Pharmacokinetic studies

Wistar rats were randomly sorted into two groups (n=12). Group I animals received drug solution (40 mg/kg) while group II was administered with Br-LPHNs (equivalent to 40 mg/kg bromelain) by oral gavage respectively. Subsequently, blood samples (250 μl) were withdrawn from rat tail vein at pre-dose (0.0), 0.5, 1, 2, 4, 6, 8, 12 and 24 h post treatment respectively. Plasma was collected by centrifuging blood at 3000 rpm for 5 min at 4°C and analyzed for bromelain's proteolytic activity corresponding to bromelain content.^{14,15} Winnonin® 6.1 (Pharsight Corporation, Mountain View, CA) pharmacokinetic software was utilized to determine various pharmacokinetic parameters using non-compartmental analysis.



Pharmacodynamics studies

View Article Online
DOI: 10.1039/D4PM00327F

Intraperitoneal injections of OVA solution (150 µg ovalbumin and 100 mg aluminum hydroxide emulsified in 1 ml of normal saline) were administered to sensitize 20 healthy guinea pigs weighing 250–300 g on first and seventh day, respectively followed by a booster dose on day 14.³⁵ Subsequently, guinea pigs were randomly assigned equally into 4 groups (n = 6). Group I animals were given normal saline, whereas groups II, III, and IV received chlorpheniramine maleate (10 mg/kg), bromelain solution (10 mg/ kg) and optimized Br-LPHNs (10 mg/kg equivalent to bromelain) for 7 days. Similar to OVA-sensitized animals, six naïve animals were sham-sensitized with normal saline.

Following seven days of sequential treatment, animals in each group were challenged with a histamine dihydrochloride solution (1% w/v). Animals' physiological reactions, survival, pre-convulsive dyspnea (PDT) and recovery time (RT) were monitored during study.³⁶ The following formula was used to calculate the percentage protection provided against asphyxia:

$$\% Protection = \frac{BT1}{BT2} \times 100 \quad (ii)$$

where BT1 denotes time at which bronchospasm began in control group and BT2 denotes time at which bronchospasm began following pretreatment with standard or test samples. Following exposure to histamine aerosols, animals were sacrificed to obtain blood samples via heart puncture and organs like trachea, liver, spleen, and lung respectively. Hematological parameters such as WBC, hemoglobin level, blood cell counts, TNF-α, IL-5, and IgG were assessed. Consequently, oxidative stress markers such as lipid peroxidation (LPO), protein carbonyl content, myeloperoxidase (MPO) activity, reduced glutathione (GSH), superoxide dismutase (SOD), catalase and nitric oxide (NO) level were estimated in tissue homogenates to assess their antigen-specific response.^{14,27}

Bronchoalveolar fluid analysis



Immediately following blood collection, trachea of sacrificed animals was carefully exposed and cannulated. Five bronchoalveolar lavages were performed by infusing normal saline through a cannula followed by aspiration after gently massaging lungs. The obtained samples were combined to calculate the total number of cells per milliliter using a Neubauer hemocytometer after staining with Giemsa stain.³⁵ Simultaneously, separated BAL fluid was evaluated for eosinophils count, immunological (TNF- α , IL-5, and IgG) as well as oxidative stress markers.

Statistical Analysis

Dunnett's post-hoc test and one-way ANOVA were used for statistical analysis in GraphPad Prism version 5.00 (GraphPad Software, California, USA). The differences were considered statistically significant in all studies at $p < 0.05$.

Results and discussion

Optimization of Br-LPHNs

Various process variables were optimized taking into account mean particle size, entrapment efficiency, PDI and zeta potential as paradigm framework. Increase in soya lecithin to drug weight ratio from 1:1 to 2:1 had positively influenced the entrapment efficiency and lowered particle size due to amphiphilic nature of soya lecithin. This might be attributed by physical adsorption of soya lecithin at the interface of primary emulsion (w/o) which hindered the permeation of drug to external aqueous phase (Table 1).³⁷ However, further increment of lipid: drug ratio (3:1) reduced entrapment efficiency with increment of particle size and PDI owing to its positive effect on matrix viscosity which might have not allowed an effective particle size reduction (Table 1).³⁸ Simultaneously, higher lipid amount also promoted the genesis and assembly of lecithin vesicles. The coexistence of lecithin vesicles might be

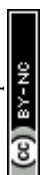


contributing to growth of particle size and lowering of their zeta potential.³⁹ In addition, the relative increment in polymer load at drug - polymer weight ratio of 1:6.67 had improved entrapment efficiency by facilitating rapid film genesis over the core material to fix the nanoparticulate structure and delayed solvent and non-solvent counter diffusion.^{29,40} However, further increase in polymer load at drug-polymer weight ratio 1:8 resulted in a lower real drug load, which in turn demonstrated reduced entrapment efficiency. Higher polymer proportion also favored the formation of coarse dispersion as illustrated by greater PDI due to lack of sufficient energy to overcome the viscous forces (Table 1).^{16,27}

Higher external phase volume remarkably increased particle size and PDI with diminution of encapsulation efficiency owing to the lack of ample shear forces for development of uniform stable micellar structures (Table 1).^{27,29}

Sonication period during primary and double emulsion preparation had a substantial impact on particle size, entrapment efficiency and colloidal properties. An increase in sonication time accelerated the production of small sized particles with higher entrapment efficiency by creating consistent micellar structures during primary (7 min) and secondary (15 min) emulsification steps, respectively. Nevertheless, further escalation of sonication duration during primary (9 min) and secondary emulsification (20 min) resulted in increased particle size and PDI with lower zeta potential and entrapment efficiency, respectively (Table 1). The disruption of interfacial barrier during micellization as a result of high shear forces might have facilitated the coalescence of dispersed phase.^{15,16}

H₄ formulation exhibiting highest entrapment efficiency ($89.94 \pm 3.98\%$) with homogeneously dispersed nanoparticles (190.91 ± 29.48 nm) was chosen for additional studies.



SEM analysis of optimized batch manifested uniform spherical shape with size around 200 nm (Fig. 1A).

Bromelain's integrity

The conformational integrity of bromelain encapsulated in nanoparticles was further evaluated by fluorescence spectroscopy. The emission spectrum of pure bromelain and bromelain released from optimized formulation revealed λ_{\max} at 330 nm corresponding to intense emission of tryptophan. However, slight decline in fluorescence intensity of bromelain leached out of optimized formulation was observed without any shift in λ_{\max} (Fig. 1B). The results confirmed that formulation parameters were suitably optimized and maintained the conformational integrity of tertiary structure of bromelain during encapsulation.⁴¹

On the contrary, pure drug incubated at simulated gastric pH showed significantly lower fluorescence intensity with shift in λ_{\max} to 343 nm. The red shift in λ_{\max} for pure bromelain incubated at pH of gastric milieu might be attributed to conformational changes in the vicinity of tryptophan surface indicating denaturation of bromelain in acidic environment.⁴² However, no change in aromatic chromophore of bromelain recovered after lysis of nanoparticulate formulation earlier incubated under simulated gastrointestinal pH was observed (Fig. 1C). The results further confirmed that structural protection offered by vesicular system helped in maintenance of tertiary structure as well as proteolytic activity of bromelain in Br-LPHNs.⁴³

Drug release

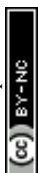
Dissolution study was executed in pH progressive media to ascertain the prospective of Br-LPHNs in modulating drug release for extending bromelain's action. Optimized formulation



at simulated gastric pH showed ~ 11 % drug release in 2 h. The desorption of surface adsorbed or weakly bound drug or partial film flaws developed during lyophilization might be contributing to such peculiar initial drug release when polymer coat remained unionized. Afterwards, a brisk increase in drug release for 2 h followed by prolonged release upto 24 h was observed as pH of dissolution media was raised to pH 6.8 to mimic the pH of small intestine (Fig. 1D). The sustained release might be attributed to hindrance furnished by lecithin and PMMA envelop to the inflow of dissolution medium and diffusion of bromelain from core.^{29,38} Furthermore, dissolution data of Br-LPHNs was fitted to different release kinetic models to ascertain the drug release mechanism. Korsmeyer-Peppas model was the best fit release model for optimized formulation as established by highest R^2 value (0.978). The release exponent's numerical value ($n = 0.73$) demonstrated that a mix of the diffusion and dissolving phenomena regulated bromelain release.

Mucolytic activity

Secretory epithelial cells typically secrete gel forming polymeric mucins, principle component of mucus. Thus, artificial mucus composed of cross-linked locust bean gum mucilage was taken to mimic similar viscoelastic behavior of real human airway mucus.⁴⁴ On exposure of artificial mucus with pure bromelain, the remarkable decrease in mucous viscosity was observed due to disruption of glycosidic bonds and splitting of protein in smaller fragments.^{45,46} Optimized formulation initially manifested lower degree of mucus liquefaction followed by robust influence on viscosity of artificial mucus similar to pure drug after 4 h (Fig. 2). Slow drug release behavior of Br-LPHNs contributed to lower mucolytic activity of formulation during initial hours. However, mucus viscosity reduced with progression of time significantly due to deeper penetration of nanoparticulate formulation in microarchitecture and mesh spacing of artificial mucus.⁴⁷ In addition, progressive release of



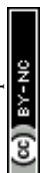
bromelain from Br-LPHNs prevented end product inhibition effect as observed in case of pure bromelain and contributed to higher mucolytic activity for longer duration.⁴⁸

Stability studies

The effect of storage conditions on proteolytic activity of pure drug and Br-LPHNs under accelerated and room temperature respectively are presented in Table 2. Pure drug under accelerated and room temperature storage conditions showed remarkable decrease in proteolytic activity expressed as drug content compared to Br-LPHNs. Bromelain followed first order degradation kinetics. Lower K_{cal} and higher calculated t_{90} value (~6.99 folds) for formulation compared to pure drug manifested significantly better stability of formulation under real time stability conditions.⁴³ Visual changes in color of pure drug from off white to brown was observed at both room and accelerated temperature storage condition respectively whereas no color change was observed for Br-LPHNs. This further indicated that formulation parameters were appropriately optimized to formulate a stable bromelain loaded nano-formulation.

Pharmacokinetic studies

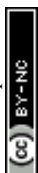
Plasma drug concentration time profile post oral administration of free drug and Br-LPHNs in wistar rats are represented in Fig. 3A. Optimized formulation after single dose administration showed significantly ($p < 0.05$) higher C_{max} (1.78-fold) compared to pure bromelain. Higher C_{max} value might be contributed by protection offered by carrier system to bromelain in gastric milieu along with absorption of nanoparticles through specific absorption mechanisms owing to their nano-size and hydrophobic surface facilitating their permeation across GIT. Delayed T_{max} (2-fold) too confirmed sustained in vivo bromelain release from optimized Br-LPHNs formulation similar to in vitro drug release study. Smaller $t_{1/2}$ and low systemic mean residence time (MRT) of pure drug indicated its faster systemic



clearance ($p < 0.05$). Besides, Br-LPHNs manifested higher $t_{1/2}$ (3.38-fold) and MRT (3.32-fold) respectively. The results revealed prolonged systemic absorption and slow release of drug from Br-LPHNs into systemic circulation. Meanwhile, AUC_{0-24h} was also significantly increased upto 6.89-fold for formulation compared to pure drug (Table 3) ($p < 0.05$). The apparent bromelain loading in LPHNs might have assisted in bypassing the extensive gut wall metabolism due to intimate association of drug with lipid polymeric shell and improved bioavailability. In addition, lymphatic uptake through specialized absorption mechanisms like paracellular and transcellular transport via endocytosis and M-cells of Payer's Patches might have ensured an increase in bioavailability.^{29,49,50}

Ovalbumin induced asthma model

During present study, OVA sensitization evoked remarkable airway hyperresponsiveness to histamine challenge.⁵¹ Bronchospasm onsets, recurrent episodes of jerk and recovery time from difficulty in breathing in response to histamine exposure were the major clinical parameters evaluated to determine efficacy of various treatments (Fig. 3B). Bronchial hyperresponsiveness in response to histamine in OVA-sensitized animals was significantly higher than normal saline sensitized animals ($p < 0.05$). Remarkable rise in span of histamine induced bronchospasm by 11.14 %, 45.08 % and 157.37 % and diminution in recovery time after bronchospasm induction by 48.14 %, 64.80 % and 82.57 % was noticed in drug, chlorpheniramine and optimized formulation treated animals respectively compared to control animals ($p < 0.05$). However, Br-LPHNs significantly suppressed bronchial hyperresponsiveness by hampering bronchospasm onset about 292.46 %, 120.69 % and 67.08 % respectively in comparison to saline treated, bromelain and chlorpheniramine treated group. Br-LPHNs offered significantly high percentage protection against asphyxia compared to pure drug and chlorpheniramine ($p < 0.05$) (Fig. 3C). Higher protective impact of Br-LPHNs might be attributed to higher systemic bioavailability of bromelain as a result of



protection provided by PMMA polymer in acidic milieu of stomach and prolonged drug release characteristic of optimized formulation.⁴⁷ Br-LPHNs nullified the histamine induced bronchoconstriction similar to chlorpheniramine indicating antihistaminic effect of bromelain.

Hematological evaluation

OVA sensitized animals showed significant elevation of total leukocyte count, eosinophils, lymphocytes, neutrophils and hemoglobin relative to naïve (Fig. 4). Increased eosinophils count confirmed the allergic inflammation accompanying bronchial hyper responsiveness.⁵³ Elevated total leukocyte and lymphocytes count further assured the inflammatory state in OVA sensitized animals. Raised WBCs count induced unrestricted release of histamine in lungs of OVA sensitized animals and thus induced runny nose and wheezing during allergen exposure.⁵⁴ Oral treatment with Br-LPHNs compared to pure drug significantly ($p < 0.05$) impeded the progression of allergen induced asthmatic condition by reducing total leukocyte, lymphocyte, neutrophils and eosinophils count respectively similar to chlorpheniramine treatment (Fig. 4). The reverse shift of hematological markers back near to normal level corresponded well with increased bioavailability of bromelain via carrier system i.e., Br-LPHNs.

Oxidative and immunological markers

Carbonylated protein, MPO and LPO are salient markers of oxidative stress exhibiting a vital role in pathogenesis of asthma. Under normal physiological condition, oxidative free radical-induced damage is prevented and terminated by endogenous enzymatic (SOD and CAT) and non-enzymatic (reduced glutathione) defensive mechanisms. OVA sensitization induced oxidative cellular stress by unbalancing the formation of free radicals and antioxidant defense, as observed by declined levels of SOD, CAT, and GSH and escalated levels of LPO,



MPO and carbonylated protein (Fig. 5).⁵⁵ The elevated total cell count (3.47-fold) in BAL fluid too assured the neutrophils and lymphocytes infiltration in the lungs which contribute to lungs inflammation, mucus production and edema.

Bromelain, chlorpheniramine as well as Br-LPHNs displayed notable alleviation of oxidative stress by attenuating LPO and carbonylated protein level in lung, BALF, liver, trachea and spleen tissues respectively ($p < 0.05$) (Fig. 5). The outcomes expressed the effectiveness of Br-LPHNs in suppressing the oxidative stress markers and amplification of antioxidant defense compared to pure bromelain and chlorpheniramine ($p < 0.05$) (Fig. 5). Such remarkably improved antioxidant activity of Br-LPHNs might be ascribed to improved lymphatic uptake of Br-LPHNs via phagocytosis and paracellular pathways along with preservation of bromelain's activity through stomach and sustained diffusion of drug from formulation.^{14,27}

In the OVA-sensitized control, an elevated NO level suggested the activation of prostaglandin synthesis and inducible nitric oxide synthase (iNOS) (Fig. 6).⁵⁶ Similarly, escalated TNF- α and IL-5 serum level stipulated formation of reactive oxygen species, NO synthesis, and neutrophil migration to tissues.⁵⁷ However, notable depletion of WBC count, MPO, NO and Ig-G, IL-6 and TNF- α level was observed with Br-LPHNs treatment compared to bromelain (Fig. 6). Thus, it can be assumed that bromelain's favorable antioxidant and anti-inflammatory benefits for the treatment of inflammatory disorders like asthma were provided by its inhibitory influence on NF- κ B overexpression and iNOS as well as enhanced expression of the Nrf2 pathway.^{19,21,58} Br-LPHNs' increased anti-inflammatory efficacy might be attributed due to better stomach stability and prolonged drug release characteristic bestowing long-term inhibitory effect on cytokine storm.

Histopathological analysis

The naïve group's lung microphotographs revealed clean alveolar sacs and no cell accumulation in the bronchiole region (Fig. 7A). On the contrary, OVA sensitized lungs had



dense cell deposition surrounding the bronchioles, blood vessels, and alveolar regions, suggesting that excessive cell infiltration caused the alveolar sacs to constrict (Fig. 7B). Lung tissue remodeling and inflammation may be caused by oxidative stress brought on by the OVA challenge.⁵⁵ Less cell aggregation surrounding the bronchioles and less thickening of alveolar septa were observed in the groups treated with bromelain and chlorpheniramine (Fig. 7C & D). However, no thickening around the bronchioles with very less accumulation of cells in formulation-treated group was observed (Fig. 7E).⁵

Conclusions

Br-LPHNs were successfully fabricated by double emulsion solvent evaporation method to establish a new therapy for allergic asthma management. Hybridization of lipid core containing drug with polymer coat via emulsification augmented higher drug load, improved bromelain gastric stability and facilitated prolonged drug release to achieve higher bioavailability and therapeutic effect. Br-LPHNs administration remarkably reduced allergen induced airway hyperresponsiveness and infiltration of inflammatory cells in lung tissues. The improved anti-inflammatory, antioxidant as well as anti-asthmatic activity mitigated by Br-LPHNs has indicated wider acceptability of formulation in treatment of asthma along with other disorders associated with oxidative stress and inflammation. However, formulation scalability along with its efficacy in clinical trials needs to be studied before successful implementation of Br-LPHNs in clinics.

Author contributions: **Manu Sharma:** Conceptualization, Methodology, Investigation, Supervision, Writing- Reviewing and Editing. **Namita Gupta:** Data curation, Investigation, Writing- Reviewing and Editing.

Conflicts of interest: The authors report no conflicts of interest.



Acknowledgement: The authors acknowledge the Department of Pharmacy, Banasthali Vidyapith (Rajasthan, India) for providing facilities to undertake this research.

References

1. K.R. Ahmadi and D.B. Goldstein, *Curr. Biol.*, 2002, 12, R702-R704.
2. C. Ober, *Immunol. Rev.*, 2011, 242, 10-30.
3. A. James and G. Hedlin, *Curr. Treat Options Allergy*, 2016, 3, 439–452.
4. I.D. Pavord, R. Beasley, A. Agusti, G. P. Anderson, E. Bel, G. Brusselle, P. Cullinan, A. Custovic, F. M. Ducharme, J. V Fahy, U. Frey, P. Gibson, L.G. Heaney, P.G. Holt, M. Humbert, C.M. Lloyd, G. Marks, F.D. Martinez, P.D. Sly and A. Bush, *Lancet*, 2018, 391, 350–400.
5. M. Tiwari, U.N. Dwivedi and P. Kakkar, *J. Ethnopharmacol.*, 2014, 153, 326–337.
6. L.M. Graham, *J. Allergy Clin. Immunol.*, 2002, 109, 560–566.
7. R. Dahl, *Respir. Med.*, 2006, 100, 1307–1317.
8. H.M. El-Laithy, A. Youssef, S.S. El-Husseney, N.S. El Sayed and A. Maher, *Drug Deliv.*, 2021, 28, 826–843.
9. F. Carmona and A.S. Pereira, *Rev. Bras. Farmacogn.*, 2013, 23, 379–385.
10. A.J. Chakraborty, S. Mitra, T.E. Tallei, A.M. Tareq, F. Nainu, D. Cicia, K. Dhama, T. Emran, J. Simal-Gandara and R. Capasso, *Life*, 2021, 11, 1–26.
11. A.R. Lam, K. Bazzi, S.J. Valle and D.L. Morris, *Case Rep. Oncolo.*, 2021, 14, 628–633.
12. S. Soheilifar, M. Bidgoli, A. Hooshyarfard, A. Shahbazi, F. Vahdatinia and F. Khoshkhoie, *J. Dent. (Tehran, Iran)*, 2018, 15, 309–316.
13. M. Azarkan, M.M. González, R.C. Esposito and M.E. Errasti, *Protein Pept. Lett.*, 2020, 27, 1159–1170.
14. M. Sharma and D. Chaudhary, *Nanomed. Nanotechnol. Biol. Med.*, 2022, 22, 102543.



15. M. Sharma and R. Sharma, *RSC Adv.*, 2018, 8, 2541-2551.
16. M. Sharma and D. Chaudhary, *Int. J. Pharm.*, 2021, 594, 120176.
17. T.C. Chang, P.L. Wei, P.T. Makondi, W.T. Chen, C.Y. Huang and Y.J. Chang, *PloS one*. 2019, 14, e0210274.
18. S. Müller, R. März, M. Schmolz, B. Drewelow, K. Eschmann and P. Meiser, *Phytother. Res.*, 2013, 27, 199–204.
19. J.R. Huang, C.C. Wu, R.C. Hou and K.C. Jeng, *Immunol. Invest.*, 2008, 37, 263–277.
20. E.R. Secor, W.F. Carson, A. Singh, M. Pensa, L.A. Guernsey, C.M. Schramm and R.S. Evid. Based Complement. Altern. Med., 2008, 5, 61–69.
21. K. Bhui, S. Prasad, J. George and Y. Shukla, *Cancer Letters*, 2009, 282, 167–176.
22. L.P. Hale, P.K. Greer, C.T. Trinh and M.R. Gottfried, *Clin. Immunol.*, 2005, 116, 135–142.
23. L. Desser, D. Holomanova, E. Zavadova, K. Pavelka, T. Mohr and I. Herbacek, *Chemother. Pharmacol.*, 2001, 47, 10–15.
24. H. Ikushima and K. Miyazono, *Nat. Rev. Cancer*, 2010, 10, 415–424.
25. L.P. Hale, *Int. Immunopharmacol.*, 2004, 4, 255–264.
26. N.N.M. Rao, S. Sharma, P. Kaduba, V. Sadhu, M. Sharma and A.V.S. Sainath, *J. Appl. Polym. Sci.*, 2020, 137, 48954.
27. M. Sharma, S. Sharma and J. Wadhawa, *Artif. Cells Nanomed. Biotechnol.*, 2019, 47, 45-55.
28. L. Sercombe, T. Veerati, F. Moheimani, S.Y. Wu, A.K. Sood and S. Hua, *Front. Pharmacol.*, 2015, 6, 286.
29. R.R. Patel, G. Khan, S. Chaurasia, N. Kumar and B. Mishra, *RSC Adv.*, 2015, 5, 76491–76506.



30. S. Shah, P. Famta, P.S. Raghuvanshi, S.B. Singh and S. Srivastava, *Colloids Interface Sci. Commun.*, 2022, 46, 100570. View Article Online
DOI: 10.1039/D4FM00327F
31. A. Bettencourt and A.J. Almeida, *J. Microencapsul.*, 2012, 29, 353–367.
32. O.H. Lowry, N.J. Rosebrough, A.L. Farr and R.J. Randall, *J. Biol. Chem.*, 1951, 193, 265–75.
33. X. Li, Z. Yang and Y. Bai, *Int. J. Biol. Macromol.*, 2018, 10, 144–156.
34. M.D. Anwarul Hasan, C.F. Lange and M.L. King, *J. Non-Newton Fluid Mech.*, 2010, 165, 1431–1441.
35. A.P. Lowe, K.J. Broadley, A.T. Nials, W.R. Ford and E.J. Kidd, *J. Pharmacol. Toxicol. Methods*, 2015, 72, 85–93.
36. G.A. Koffuor, A. Boye, S. Kyei, J. Ofori-Amoah, E. Akomanin Asiamah, A. Barku, J. Acheampong, E. Amegashie and A. Kumi Awuku, *Pharm. Biol.*, 2016, 54, 1354–1363.
37. R. Pichot, R. L. Watson and I.T. Norton, *Int. J. Mol. Sci.*, 2013, 14, 11767–11794.
38. M.A. Schubert and C.C. Müller-Goymann, *Eur. J. Pharm. Biopharm.*, 2005, 61, 77–86.
39. L. Zhang, J.M. Chan, F.X. Gu, J.W. Rhee, A.Z. Wang, A.F. Radovic-Moreno, F. Alexis, R. Langer and O.C. Farokhzad, *ACS Nano.*, 2008, 2, 1696–1702.
40. M. Sharma, V. Sharma, A.K. Panda and D.K. Majumdar, *Pharm. Dev. Technol.*, 2013, 18, 560–569.
41. A.B.T. Ghisaidoobe and S.J. Chung, *Int. J. Mol. Sci.*, 2014, 15, 22518–22538.
42. S. K. Haq, S. Rasheedi and R.H. Khan, *Eur. J. Biochem.*, 2002, 269, 47–52.
43. M. Sharma, V. Sharma, A.K. Panda and D.K. Majumdar, *Int. J. Nanomed.*, 2011, 6, 2097–2111.



44. H.L. Jian, X.J. Lin, W.A. Zhang, W.M. Zhang, D.F. Sun and J.X. Jiang, *Food Hydrocoll.*, 2014, 40, 115–121.
45. K. Pillai, J. Akhter, T.C. Chua and D.L. Morris, *Int. J. Cancer Res.*, 2014, 134, 478–486.
46. S.L. Wang, H.T. Lin, T.W. Liang, Y.J. Chen, Y.H. Yen and S.P. Guo, *Bioresour. Technol.*, 2008, 99, 4386–4393.
47. C. Müller, K. Leithner, S. Hauptstein, F. Hintzen, W. Salvenmoser and A. Bernkop-Schnürch, *J. Nanoparticle Res.*, 2013, 15, 1-13.
48. M. Sharma, V. Sharma and D.K. Majumdar, *Int. Sch. Res. Notices*, 2014, 2014, 1–8.
49. W. Wang, R. Zhu, Q. Xie, A. Li, Y. Xiao, K. Li, H. Liu, D. Cui, Y. Chen and S. Wang, *Int. J. Nanomedicine*, 2012, 7, 3667–3677.
50. G. Sahay, D.Y. Alakhova and A.V. Kabanov, *J. Control. Release*, 2010, 145, 182–195.
51. V. Zugic, N. Mujovic, S. Hromis, J. Jankovic, M. Drvenica, A. Perovic, I. Kopitovic, A. Ilic and D. Nikolic, *J. Clin. Med.*, 2018, 7, 1–9.
52. P.J. Mauser, A. House, H. Jones, C. Correll, C. Boyce and R.D. Chapman, *Pulm. Pharmacol. Ther.*, 2013, 26, 677–684.
53. K. Nakagome and M. Nagata, *Front. Immunol.*, 2018, 9, 2220.
54. T. Hailemaryam, W. Adissu, L. Gedefaw and Y. Asres, *Hematol. Transfus. Int. J.*, 2018, 6, 77–82.
55. A.O. Antwi, D.D. Obiri and N. Osafo, *Mediat. Inflamm.*, 2017, 1-11.
56. A. Hori, M. Fujimura, N. Ohkura and A. Tokuda, *Cough*, 2011, 7, 5.
57. Z. Cai, J. Liu, H. Bian and J. Cai, *Am. J. Transl. Res.*, 2019, 11, 7300–7309.
58. K. Bhui, S. Tyagi, A.K. Srivastava, M. Singh, P. Roy, R. Singh and Y. Shukla, *Mol. Carcinog.*, 2012, 51, 231–243.

New Article Online
DOI: 10.1059/D4PM00327F



Table 1: Effect of distinct processing variables on quality parameters like size, PDI, zeta potential and entrapment efficiency.

Formulation code	Polymer (mg)	Soya lecithin (mg)	Drug (mg)	Sonication time		Continuous phase volume (ml)	Particle Size (nm \pm SD)	PDI (PDI \pm SD)	Zeta potential (mV \pm SD)	Entrapment efficiency (% \pm SD)
				Pre time	Post time					
H ₁	200	25	25	7	15	30	286.43 \pm 38.61	0.18 \pm 0.01	-10.46 \pm 1.87	63.05 \pm 2.31
H ₂	200	50	25	7	15	30	230.56 \pm 25.25	0.25 \pm 0.01	-20.06 \pm 1.90	72.13 \pm 2.09
H ₃	200	75	25	7	15	30	375.33 \pm 42.61	0.39 \pm 0.01	-8.36 \pm 1.45	66.32 \pm 2.23
H ₄	200	50	30	7	15	30	190.91 \pm 29.48	0.14 \pm 0.02	-28.30 \pm 2.08	89.94 \pm 3.98
H ₅	200	50	50	7	15	30	292.23 \pm 30.50	0.18 \pm 0.01	-14.16 \pm 3.66	76.38 \pm 2.51
H ₆	200	50	30	7	15	40	314.83 \pm 42.55	0.28 \pm 0.02	-18.67 \pm 1.11	78.64 \pm 3.11
H ₇	200	50	30	5	15	30	642.9 \pm 68.25	0.67 \pm 0.05	-15.78 \pm 2.00	60.29 \pm 5.29
H ₈	200	50	30	9	15	30	328.83 \pm 45.63	0.27 \pm 0.01	-29.33 \pm 1.20	66.12 \pm 5.66
H ₉	200	50	30	7	20	30	449.2 \pm 36.39	0.32 \pm 0.01	-31.73 \pm 1.37	63.34 \pm 7.63



Table 2: Effect of storage conditions on percentage bromelain content of pure drug and Br-LPHNs.

Storage condition	Sample	Bromelain activity remaining (% ± SD)							t ₉₀ (days)
		0 M	1.5 M	3 M	6M	9M	12 M	Kcal (days ⁻¹)	
25±2°C/60 ±5% RH	Bromelain	100.00±1.23	95.45±2.34	90.46±1.11	85.86±1.90	81.23±2.34	73.12±4.32	8.06 X 10 ⁻⁴	129.02
	H ₄	100.00±2.72	99.09±3.67	98.88±2.05	97.81±1.86	96.81±2.05	95.36±3.84	1.15 X 10 ⁻⁴	903.16
40±2°C/75 ±5% RH	Bromelain	100.00±1.23	89.45±3.90	85.90±2.50	74.18±1.79			1.59 X 10 ⁻³	65.44
	H ₄	100.00±2.72	98.26±3.01	98.73±3.99	94.77±5.26			2.76 X 10 ⁻⁴	376.51

Values are expressed as mean ± SD, Abbreviations: M= month; Kcalc = calculated first order degradation rate constant; t₉₀ = time to reach 90% of initial drug concentration



Table 3: Pharmacokinetic parameter of pure drug and optimized formation obtained after oral administration. View Article Online
DOI: 10.1039/D4PM00327F

oral administration.

Parameter	Pure drug	Formulation
C _{max} (ng ml ⁻¹)*	4.02 ± 1.09	7.18 ± 2.90
T _{max} (h)*	2.00 ± 0.11	4.00 ± 0.21
K _e (h ⁻¹)*	0.33 ± 0.11	0.08 ± 0.01
t _{1/2} (h)*	2.11 ± 0.32	7.51 ± 0.51
MRT (h)*	3.18 ± 0.49	10.58 ± 0.93
AUC (ng h ² ml ⁻¹)*	15.58 ± 3.22	107.50 ± 13.12
Relative bioavailability (%)		689.99

#Values are expressed as mean ± SD, n=3; * p<0.05 level of significant difference



Fig. captions

Fig. 1: (A) Scanning electron microscopy photograph of optimized formulation (H₄), Fluorescence spectra of (B) pure drug and (C) bromelain released from Br-LPHNs respectively, (D) Dissolution profile of H₄ formulation in pH progressive dissolution media.

Fig. 2: Effect of pure drug solution and Br-LPHNs at an equivalent amount of 0.2 % w/w bromelain at varying time intervals on viscosity of artificial mucous respectively.

Fig. 3: (A) Plasma drug concentration time profile of bromelain solution and Br-LPHNs respectively. Effect of bromelain, Br-LPHNs and chlorpheniramine maleate on (B) bronchospasm onset time, recovery time, convulsion period and (C) % protection respectively.

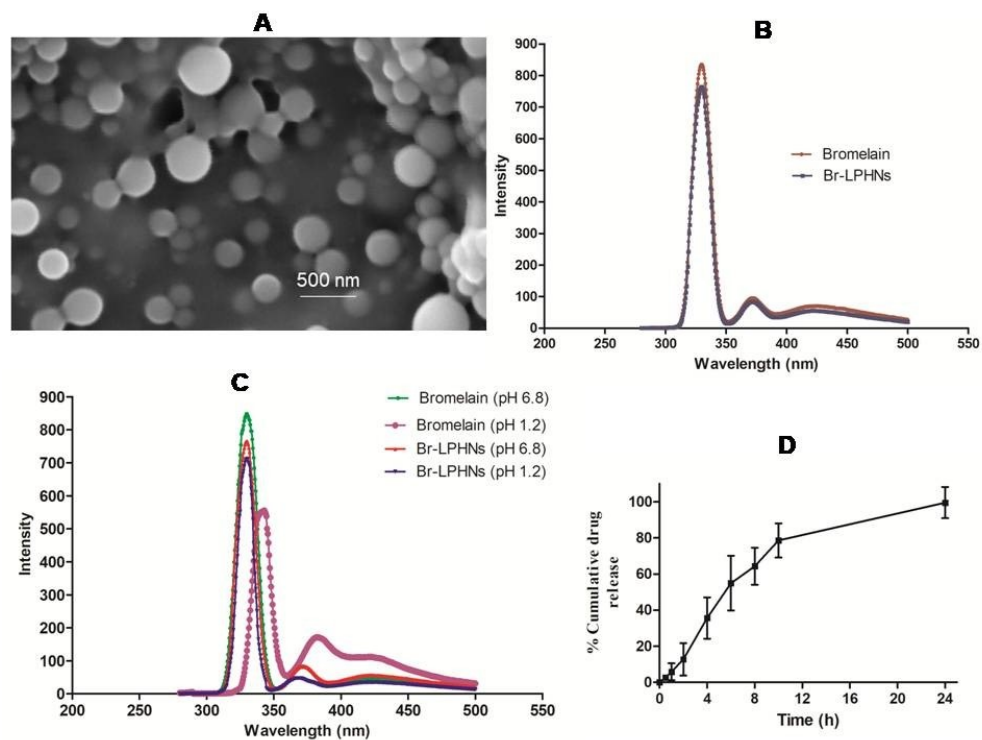
Fig. 4: Hematological biomarkers profile of different groups of animals (A) hemoglobin content, (B) total leucocyte count, (C) neutrophil (%), (D) eosinophil (%) and (E) lymphocyte (%) respectively.

Fig. 5: Effect of different treatments on level of (A) LPO, (B) carbonylated protein, (C) MPO and antioxidant biomarkers i.e., (D) catalase, (E) GSH and (F) SOD activity respectively; (G) BAL total cell and (F) BAL eosinophil count respectively.

Fig. 6: Assessment of changes in immunological biomarkers like (A) NO in tissue homogenates; (B) TNF- α , (C) IL-5 and (D) Ig-G in serum and BALF respectively in different test group animals.

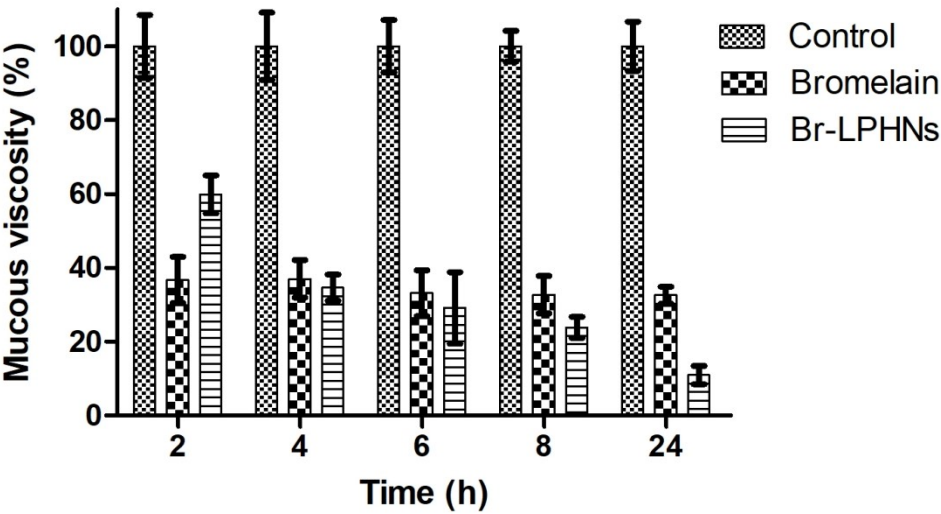
Fig. 7: Microscopic images of lung sections from saline sensitized guinea pigs (A, naïve) and ovalbumin sensitized (B) saline, (C) bromelain, (D) chlorpheniramine and (E) Br-LPHNs treated animals respectively.



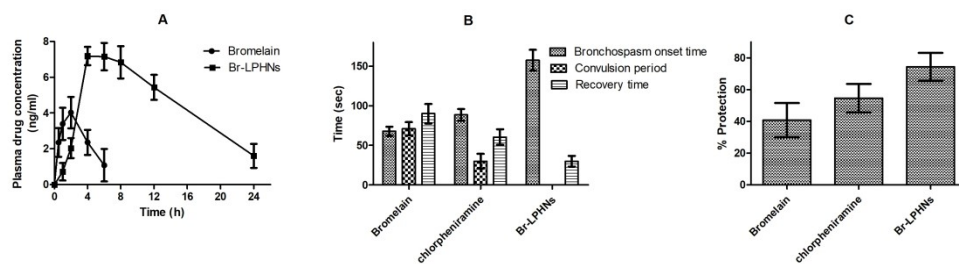


254x190mm (96 x 96 DPI)



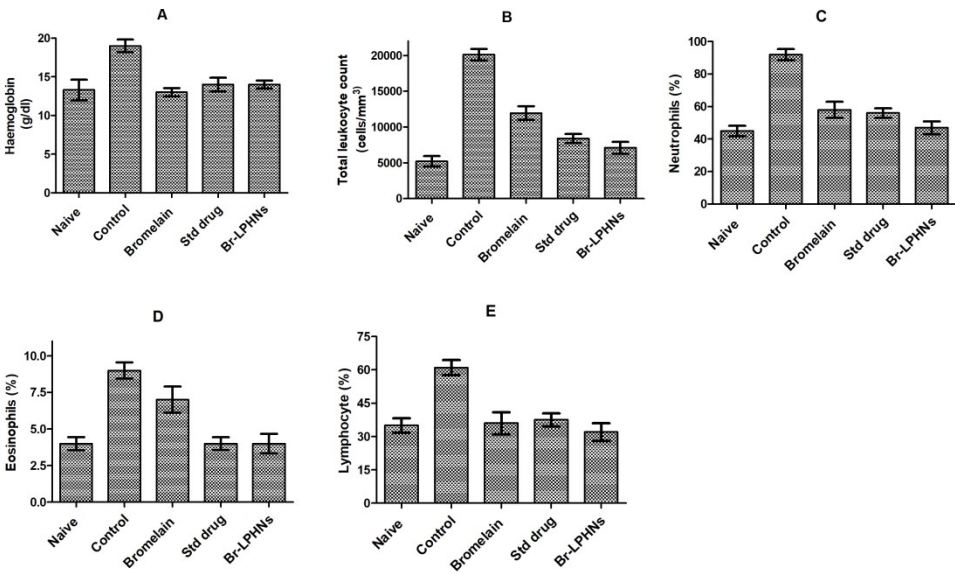


124x73mm (300 x 300 DPI)



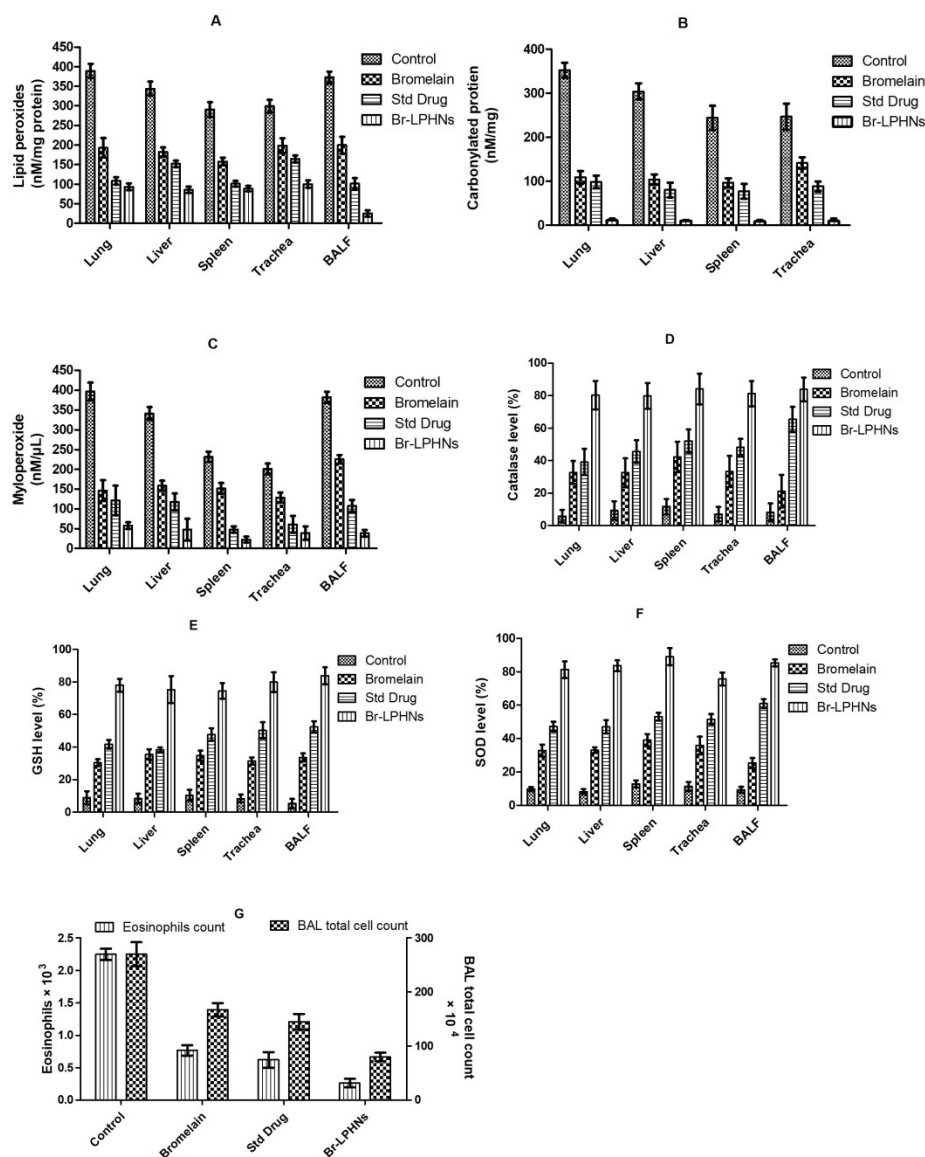
266x84mm (300 x 300 DPI)





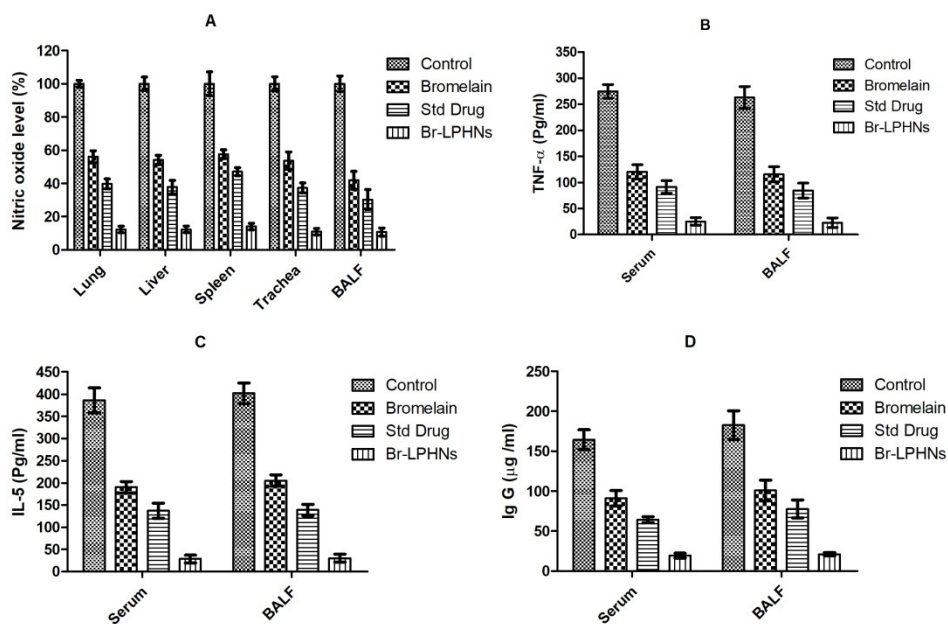
257x158mm (300 x 300 DPI)





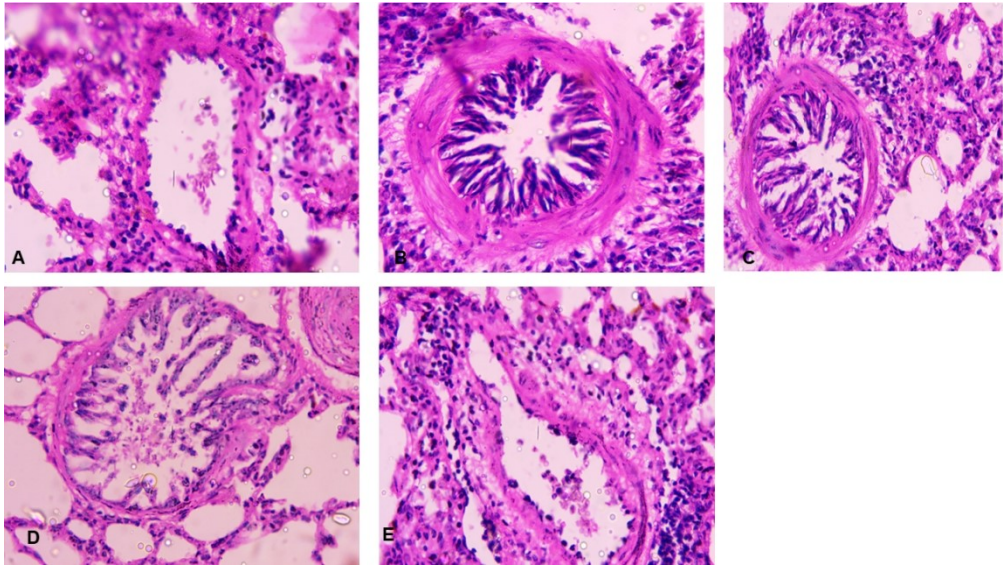
212x261mm (300 x 300 DPI)





213x148mm (300 x 300 DPI)





338x190mm (96 x 96 DPI)



Data availability: The datasets generated during and/or analysed during the current study are available from the corresponding author on reasonable request.

